AFM and FTIR Spectroscopy Investigation of the Inverted Hexagonal Phase of Cardiolipin

Andrea Alessandrini*,†,§ and Umberto Muscatello‡,§

Department of Physics, University of Modena and Reggio Emilia, Via Campi 213/A, I-41100, Modena, Italy; Department of Biomedical Sciences, University of Modena and Reggio Emilia, Via Campi 287, I-41100, Modena, Italy; and CNR-INFM-S3 National Center on Nanostructure and BioSystems at Surfaces, 41100 Modena, Italy

Received: November 3, 2008; Revised Manuscript Received: January 15, 2009

Atomic force microscopy (AFM) and FTIR spectroscopy techniques have been exploited to investigate the inverted hexagonal phase (H_{II}) of cardiolipin obtained by dehydration of a phospholipid water dispersion on a solid support. The characteristic cylinders of the H_{II} phase have been imaged by AFM and the effects of different preparation conditions (temperature and the presence of chemicals) on the structural parameters and on the presence of local nanoscale defects have been studied. It has been found that the measured repeat spacing of the H_{II} cylinders decreases upon increase of temperature and addition of pentachlorophenol (PCP), a chemical which is known to affect the structure and function of lipid bilayers. It has been shown that AFM can help in revealing some features of the mechanism of the inverted hexagonal phase formation, corroborating the results of a recent molecular dynamics study on the H_{II} phase formation from multilamellar phospholipid structures.

Introduction

Phospholipids are known to adopt different structural phases depending on temperature, ionic strenght, pH, or hydration level.[1] The particular adopted phase depends in fact on a subtle balance of interactions between the hydrophobic and polar components of phospholipids with themselves and with the solvent. Among the different phases, nonbilayer ones have attracted much attention since their discovery[2] because they are considered to be relevant to many biomembrane functional processes[3] and, in particular, they are related to the membrane fusion process. Moreover, even if the presence in vivo of nonbilayer phases may remain questionable, the presence in biological membranes of phospholipids which have a tendency to adopt nonbilayer phases is relevant for biological functions, including the possibility to modulate the function of peripheral and membrane proteins.[4] On the molecular scale, the polymorphic behavior of phospholipids can be understood on the basis of the critical packing parameter S,[5] which is expressed as the ratio between the volume of the hydrophobic lipid tail (V) and the product of the cross-sectional lipid head area (A) and the critical lipid chain length (l): $S = V/(Al)$. The value of S determines the polymorphism of the aggregate: if S is lower or equal to 1 the lipids aggregate in bilayers, whereas, if S is higher than 1 they tend to aggregate in a nonbilayer phase. In terms of monolayers, a value of S different from 1 leads to a spontaneous curvature of a phospholipid monolayer, introducing the concept of "intrinsic radius of curvature" which refers to the radius of curvature of the lipid−water interface with the lipid layer in an elastically relaxed configuration.[6] In a single-component phospholipid bilayer phase, even if the single monolayers would prefer separately a curled conformation, under specific conditions, a planar configuration is adopted, giving rise to a state of physical frustration inside the bilayer. Any environmental variation which may induce an alteration of the S value can produce a phase transition of the lipid aggregates to a new and more stable configuration. The variations include pH, temperature, ionic strength of the solution, and hydration level. In particular, phospholipid molecules characterized by an overall conical shape in which the effective volume of the hydrophobic region is bigger than the polar region have the tendency to adopt the inverted hexagonal phase (H_{II}), characterized by a monolayer negative curvature. In this phase, the lipid molecules are arranged in cylindrical structures where the hydrophilic polar groups surround an inner aqueous core and the hydrocarbon tails fill the interstitial regions of the lattice, thus stabilizing the overall structure by the hydrophobic interactions.

A possible biological function of lipid nonlamellar phases was originally hypothesized to account for the presence in biological membranes of a significant number of lipids prone to form nonlamellar phases.[7−10] In recent years, the tendency of a membrane to form nonlamellar phases has emerged as a fundamental property central for a variety of important cellular events. These include the process of membrane fusion,[11−13] the interaction of heterotrimeric G proteins with the membranes in signal progression[14,15] and the acquisition of antigenic properties.[16] Moreover, it has been shown that the efficiency of important therapeutic procedures, such as gene transfection, gene silencing, and drug delivery, is related to the transition of the lipid carrier to the hexagonal phase.[17,18]

Many different techniques have been exploited to study the lipid polymorphism. Among them, X-ray diffraction[2] and electron microscopy[19] reveal the structural parameters of the phase, calorimetry gives information on the thermodynamics of phase transitions,[20] NMR sheds light on lipid dynamics and symmetry,[21] and infrared spectroscopy[22] reveals specific chemical group changes in the absorption behavior which are related to phase changes.

* To whom correspondence should be addressed. Fax: 0039 051 2055651. E-mail: andrea.alessandrini@unimo.it.
† Department of Physics, University of Modena and Reggio Emilia.
§ National Center on Nanostructure and BioSystems at Surfaces.
‡ Department of Biomedical Sciences, University of Modena and Reggio Emilia.

10.1021/jp809705d CCC: $40.75
Published on Web 02/25/2009

Atomic force microscopy (AFM) has emerged as a promising technique in the study of solid supported lipid model membranes.[23] It has been used to study gel to liquid phase transition of supported lipid bilayers[24] and the pretransition ripple phase of specific phospholipids.[25] AFM offers the unique advantage of allowing high spatial resolution in different environment conditions (air, liquid, or controlled atmosphere) with very little disturbance on the sample, which has not to be prepared with the use of stainings to enhance the contrast. With respect to other structure determining technique AFM allows imaging in the direct space without averaging over large areas, enabling the possibility of identifying local nanoscale domains and defects.[26] However, it is worthwhile remembering that the AFM is a surface sensitive technique, so the three-dimensional structure of the sample under investigation is not always easy to deduce.

The present work aims at investigating by AFM and attenuated total reflection-FTIR (ATR-FTIR) the inverted hexagonal phase adopted by cardiolipin as a function of physical and chemical factors that control the polymorphic phase behavior of this phospholipid. It is well-known that cardiolipin, which has to accommodate four acyl chains, is among the phospholipids which, in particular conditions, adopts a nonbilayer configuration.[27] The transition from a lamellar phase to an inverted hexagonal phase may be induced for example by temperature, the presence of Ca^{2+} or other divalent cations, or dehydration of the lipid aggregates. It has been shown that the last situation, which is usually described in terms of the number of water molecules for lipid molecule, can be considered analogous to the addition of divalent cations. On the other hand, the H_{II} phase propensity of cardiolipin is thought to play a role in biological membrane function, since cardiolipin, like other anionic phospholipids, exerts its crucial effects through both its interaction with proteins and its contribution to the physical properties of the lipid phase of the membranes.[28] It is worth noting that cardiolipin contributes to modulate the surface properties of membranes. By this mechanism, cardiolipin is involved in the control of the absorption of peptides and soluble proteins onto the surface of the membranes. Conditions that perturb and/or dehydrate the interfacial region of cardiolipin aggregates including temperature variations or binding of an enzyme protein[29] may affect a range of cellular processes, such as protein translocation, electron shuttle between soluble electron transfer proteins, and membrane-bound electron transfer complexes.

In this study, we have performed a detailed study on the structural parameters of the inverted hexagonal phases adopted by cardiolipin upon dehydration on a solid support as a function of the preparation temperature and the presence in the liquid crystals of pentachlorophenol (PCP), a chemical which is known to affect the structure and function of lipid bilayers.[30] The potentiality of the AFM to give information on the local presence of defects at the nanoscale has been exploited. The obtained results have been thoroughly discussed on the basis of recently performed molecular dynamics studies on the transition between bilayer to inverted hexagonal phase of phospholipids.[13] Some aspects of the lipid aggregates have been investigated also by ATR-FTIR and FTIR spectroscopy, and the obtained results have been compared to the information derived from AFM images.

The present observations may help to explore the unique role of cardiolipin in modulating the stability and function of integral proteins in energy-transducing membranes.[28] Evidence from crystallography revealed that all of the oxidative phosphorylation complexes (including cytochrome oxidase, ATP/ADP exchange protein, FoF1ATPsynthase; cytochrome bc_1 complex, orthophosphate transporter) bind specifically to cardiolipin.[31] However, the functional effects of binding on the protein molecules, is still open to questions. In cardiolipin-lacking yeast mitochondria it has been found that mutant mitochondria are completely uncoupled at 40 °C in contrast with wild-type mitochondria that are still coupled at that temperature. This suggests that cardiolipin ensures the overall structural stability of the oxidative phosphorylation chain.[32]

Experimental Methods

Chemicals. Beef heart cardiolipin (tetraacyldiphosphatidylglycerol) (sodium salt in ethanol solution, 4.8 mg/ml) and pentachlorophenol (PCP) were purchased from SIGMA Chemical (St. Louis, MO). All the chemicals used were of the highest purity available.

Sample Preparation. Aliquots of ethanol solution of cardiolipin (tetraacyldiphosphatidylglycerol) were rotatory evaporated to dryness in glass tubes under a gentle nitrogen flux resulting in the formation of a thin film on the wall of the tube. Traces of solvent were removed in vacuo for 3 h. The solvent-free film was then hydrated in distilled water (final concentration 1 mg/mL) and dispersed by sonication for 10 min in an ice−water bath under a nitrogen stream. The lipid suspension sonication results in small unilamellar vesicles with a diameter in the range 30−50 nm. For AFM investigation, a drop of newly prepared suspension was placed onto a freshly cleaved mica surface and dried under nitrogen atmosphere. When studying the effect of temperature variations on the structural parameters of the phospholipid phase, the solvent-free film of cardiolipin, prepared as above, was hydrated in distilled water and sonicated under nitrogen stream at the temperature of interest. The suspension was then placed on the mica surface kept at the same temperature and dehydrated under a nitrogen flux. The sample was then examined with AFM at room temperature. To study the effects of pentachlorophenol on defect formation, a water solution containing 25 μM pentachlorophenol (PCP) was used to suspend the solvent-free film of cardiolipin. The procedure for cardiolipin suspension and sample preparation was as above. For ATR-FTIR investigation samples were prepared by spreading the aqueous lipid dispersion on one side of the ATR crystal and letting the solvent to slowly evaporate under a nitrogen stream. The thickness of the sample on the crystal was above the limit which allows to use the thick film approximation for calculating the order parameters. Both nonpolarized and polarized spectra were obtained and, in the latter case an order parameter for the sample under investigation was calculated according to eq 1.

Atomic Force Microscopy (AFM). The AFM observations were made by a Veeco Nanoscope IIIA Multimode, equipped with a 16×16 μm^2 scanner, operated in tapping mode in air. Silicon-etched cantilevers (resonance frequency about 300 kHz) were used for tapping mode. To study cardiolipin samples deposited on the silicon crystal for IR analysis, a Bioscope microscope (Veeco) with the same controller was used. The imaging force was reduced at the minimum in order to make negligible the perturbation on the original molecular lattice. Images were acquired at different scanning rate and magnification to be sure that the observed features and repeats were not due to noise. Some of the AFM images are visualized in the error mode[33] in order to highlight the height variation features. The quantitative and crystallographic analysis was performed by fast Fourier transform (FFT) of high-resolution images.

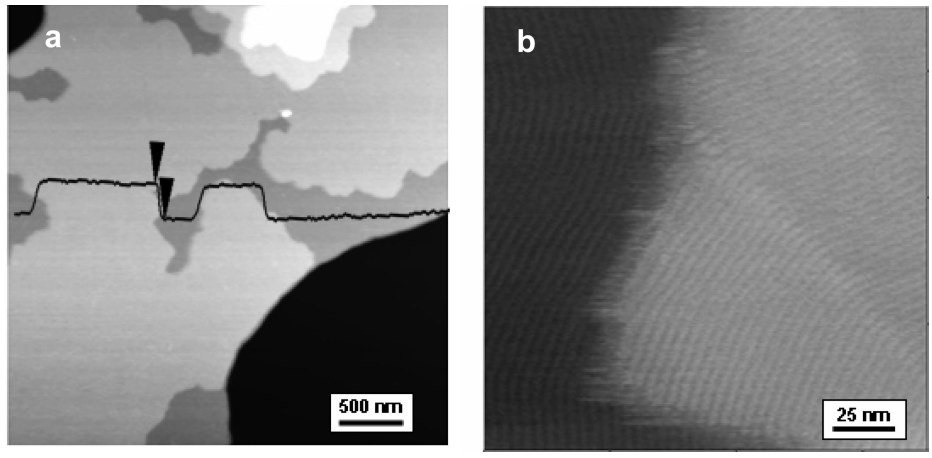

Figure 1. (a) AFM low-resolution image of a cardiolipin water solution dehydrated on a mica surface. The black line represents a height section along a horizontal line. The height difference between the two arrows is 3.9 nm. (b) Higher resolution image of the same sample in (a): the presence of parallel cylinders on the crystal surface is evident.

FTIR spectroscopy. For FTIR measurement a Jasco 470 Plus spectrometer equipped with a DTGS detector was used. Spectra were acquired by averaging 256 acquisitions at 4 cm^{-1} resolution. A silicon parallelogram crystal (80 × 10 × 5 mm^3) cut at 45° angle was used to work in the attenuated total reflection (ATR) mode allowing a total of 20 reflections. A CaF_2 window with a gold wire grid was used to linearly polarize the IR beam. Absorbance spectra of the sample were calculated using the respective spectra of the bare ATR silicon crystal obtained in the single beam mode as background. Before each measurement the silicon crystal was exposed to a piranha solution (1:3, H_2O_2:H_2SO_4), washed extensively with bidistilled water (18 MΩ cm), and exposed to an oxygen plasma discharge in a plasma cleaner. This cleaning procedure assured a hydrophilic surface to the ATR crystal.

The order parameter for the lipid film has been determined according to

$$S = \frac{2(E_x^2 - R^{ATR}E_y^2 + E_z^2)}{[(3\cos^2\alpha - 1)(E_x^2 - R^{ATR}E_y^2 - 2E_z^2)]} \quad (1)$$

where R^{ATR} is the measured linear dichroic ratio resulting from the ratio between the absorption maximum at parallel polarization ($A^{\parallel}$) and at perpendicular polarization ($A^{\perp}$); E_x, E_y, and E_z are the electrical field amplitudes on the Si interface calculated in the limit of thick sample[34] assuming a refractive index for the lipids $n_{lip} = 1.43$, and α is the angle between the transition dipole moment responsible for the observed absorption peak and the molecular axis which is assumed to be 90° for the CH stretching vibrations. In general, polarizers used for IR studies present some leakage and are not able to polarize the light to 100%. To take into consideration this aspect, we measured the polarization efficiency on pure liquid water for which the OH stretching vibration can be considered isotropic.[35] We obtained a dichroic ratio for water of 1.93, corresponding to a polarization leak of 0.035. To compare the amount of residual water in the H_{II} phase structures obtained at different temperature, the OH stretching absorption region was analyzed using a nonpolarized IR beam in ATR. Transmission FT-IR was performed by the same spectrometer on samples dehydrated on a silicon substrate.

Results and Discussion

In the absence of divalent cations, cardiolipin in excess water forms the familiar multilamellar bilayer phase in which a sequence of water layers and bimolecular lipid leaflets is found. In the presence of divalent cations such as Ca^{2+} or Mg^{2+} or Ba^{2+}, the self-organization of cardiolipin molecules gives rise to the inverted hexagonal phase (H_{II}) which is characterized by lipid molecules arranged in cylindrical structures where the hydrophilic polar groups surround an inner aqueous core and the hydrocarbon tails fill the interstitial regions of the lattice, thus stabilizing the overall structure by the hydrophobic interactions. The effect of the divalent cations consists in screening the electric charges carried out by the phosphate groups causing a sensible reduction of the effective area occupied by the polar groups and an increase of the volume of the hydrophobic part of the molecule with respect to the hydrophilic one. The effect of the divalent cations can be considered equivalent to a dehydration of the lipids from a structural point of view.[27] In fact, the removal of water causes the transition of the bilayer organization of cardiolipin into the inverted hexagonal phase. This is due to the fact that as the headgroup hydration level decreases, it becomes impossible for the lipids to maintain their lamellar packing. In this case all the remaining water is sequestered in the core of the inverted cylindrical structures of the H_{II} phase with the hydrophobic acyl chains preferring to be exposed to the apolar environment. The phenomenon is well established by X-ray diffraction,[27] but it is not evident at first sight by AFM. This is illustrated in Figure 1 which shows a typical AFM image of a sample of cardiolipin water dispersion placed on a mica surface and dehydrated by a nitrogen flux. Examination at low magnification shows that cardiolipin molecules are assembled as to form (flat) layers (sheets) having a height of 3.9 ± 0.1 nm (Figure 1a). At higher resolution (Figure 1b) each layer (sheet) appears to be formed by linear stripes, regularly spaced from each other by a repeat spacing R_p of 4.7 ± 0.1 nm and lying parallel to the mica substrate. The value of the repeat spacing does not change by exposing the sample to longer periods of nitrogen flux, indicating that the sample is in a stable configuration as far as the water-to-lipid molecular ratio is concerned.

Assuming that, under the conditions of dehydration used, cardiolipin self-assembles according to the H_{II} phase, as demonstrated by X-ray diffraction, the images suggest that the AFM tip is tracing the hydrophobic region of hexagonally organized cylinders. This is further supported by geometrical considerations on the ratio between the lateral repeat spacing R_p and the height difference between layers. As a consequence of the strong amphiphilic character of cardiolipin, the polar heads

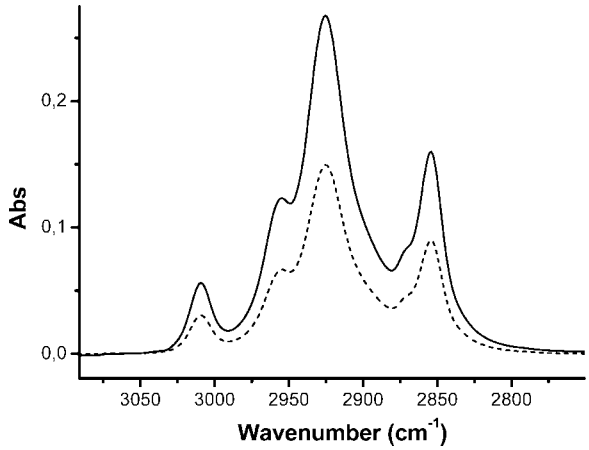

Figure 2. ATR-FTIR polarized spectra in the CH stretching region of a cardiolipin sample dehydrated on the silicon surface for the parallel polarization (solid line) and for the perpendicular polarization (dashed line).

of the first layer of molecules in contact with the support, are oriented toward the mica surface and interact with its charges whereas the alkyl chains are oriented almost perpendicularly to the surface.[26] The hydrophobic surface thus formed allows the formation of the cylindrical structures (inverted hexagonal phase) and its stabilization by hydrophobic interactions.

The conclusion that, under the conditions used, cardiolipin molecules aggregate according to the H_{II} phase is further supported by evidence obtained from polarized ATR-FTIR technique. The analysis by AFM of samples prepared for ATR-FTIR examination, i.e., directly on ATR crystal, shows the same pattern of molecular self-aggregation as that seen in the case of molecules aggregated on mica surface. Moreover, the study by AFM provides the measurement of sample thickness, a condition essential to ensure that the whole evanescent field of IR radiation is inside the sample (~250 nm at 3000 cm^{-1}). In fact, this condition is required for using the thick-sample hypothesis to determine the order parameter from the measured dichroic ratio (see eq 1). As regards the order parameter of the acyl chains, two limiting cases can be considered: (i) the lipids are organized in a bilayer configuration with the hydrophobic chains almost perpendicular to the ATR crystal surface, and (ii) the lipids are organized in the inverted hexagonal phase with the cylinder axes parallel to the ATR surface. In this second case, if the occurrence of domains with different orientation allows a uniform distribution of the cylinder directors over all directions parallel to the crystal surface, an order parameter around 0 is expected.[36] A contribution from the first cardiolipin layer in direct contact with the hydrophilic silicon surface and with the lipid headgroups in contact with the surface can be neglectd.

Figure 2 reports the IR spectra in the CH stretching region of the cardiolipin samples obtained with the parallel and perpendicular polarization of the beam. The absorption spectra are characterized by two intense bands corresponding to the asymmetric (ν_{as}) and symmetric (ν_s) CH_2 stretching vibrations at 2925 and 2854 cm^{-1}, respectively, and two shoulders at 2874 and 2956 cm^{-1} due to the symmetric and antisymmetric CH_3 stretching mode, respectively. Moreover, due to the high degree of unsaturation of the acyl chains, an absorption peak at 3010 cm^{-1} is evident and represents the ν_{as}(=CH). The high frequency values of the CH stretching absorption peaks are consistent with a high degree of gauche conformers in the methylene groups of the acyl chains.[37] This could be interpreted by the increased free volume existing in the hydrophobic region of the H_{II} phase.

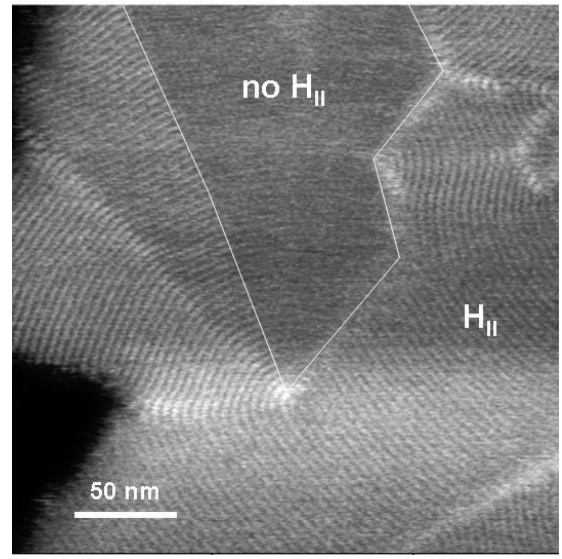

Figure 3. AFM image of a cardiolipin sample dehydrated on a mica substrate at 32 °C. Coexisting areas of inverted hexagonal phase (H_{II}) and no-H_{II} phase are clearly seen. Moreover, different H_{II} domains are seen separated by domain boundaries forming 60° and 120° angle between each other (white line overlaid).

However, from the absolute value of the absorption frequency, no direct correlation with the number of gauche bonds can be established. The linear dichroic ratio measured at 2854 cm^{-1} is 1.85 which translates in an order parameter of 0.1 according to eq 1. The low order parameter suggests a uniformly distributed direction of the induced dipole moment of the CH groups accordingly to an inverted hexagonal phase.

The AFM inspection shows that, although the majority of present domains is in the H_{II} phase organization, some well-defined areas in which the H_{II} phase has not been established can be recognized (Figure 3). The coexistence of different phases in the same specimen indicates that there are areas of the specimen in which the transition to the H_{II} phase has not been completed.

Besides the lipid-to-water molecular ratio, an important factor that definitely influences the mode of lipid self-assembling is the temperature. The phase behavior of cardiolipin−water systems was therefore studied as a function of temperature analyzing different samples prepared by isothermal dehydrations at various temperatures. To this aim, an aliquot of dried cardiolipin was suspended in water at a given temperature in a nitrogen atmosphere. A drop of suspension was then placed on a mica surface kept at the same controlled temperature and dehydrated by a nitrogen flux. The sample was immediately observed by AFM operating at room temperature. Even if the imaging temperature was different from the preparation temperature, in our case we can assume that the sample, once prepared, is in a stable configuration and the obtained results are self-consistent. This could not be the case for other lipid systems. This preparation strategy allows to study the effect of the temperature on the lyotropic phase transition of cardiolipin in water. The temperature at which the cardiolipin molecules self-aggregate influences both the lattice parameters and the formation of defects in the crystal structures. AFM examination reveals that, under the conditions of dehydration used, the cardiolipin molecules assemble in the inverted hexagonal phase at all temperatures investigated from 5 to 39 °C. The cylinder repeat spacing decreases by about 0.1 nm by varying the preparation temperature from 25 to 39 °C (Table 1). The extent

TABLE 1: Cylinder Repeat Spacing As a Function of Temperature for Cardolipin Crystals Dehydrated on a Mica Surface

temp (°C)	lattice type by AFM	cylinder repeat spacing (nm)[a]	notes[b]
5	straight cylinders	4.3	absence of domains
25	straight cylinders	4.7	absence domains
32	straight cylinders with grain boundaries	4.7	presence of domains
39	curvilinear cylinders	4.6	presence of focal domains

[a] The quantitative data of the cylinder repeat spacing were obtained by FFT of the images. The differences were statistically significant. [b] The presence or absence of domains refers to images obtained on a scan area of 400 × 400 μm^2.

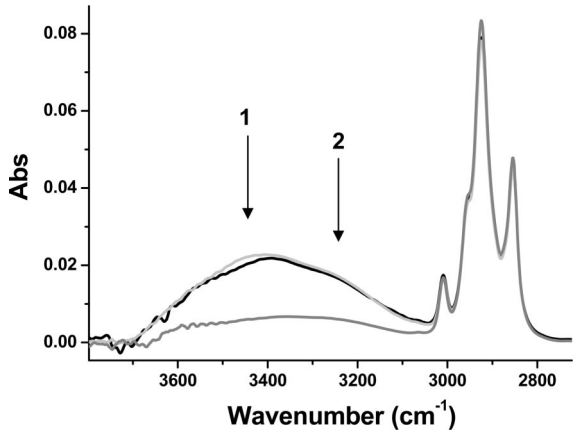

Figure 4. ATR- FTIR spectra of cardiolipin samples dehydrated at different temperatures on the silicon ATR crystal (gray 38 °C, light gray 23 °C, black 5 °C) in the OH and CH stretching regions. The arrows point to the contribution of the water-like oscillator strength (1) and ice-like oscillator strength (2).

of the decrease corresponds to a gradient of about 0.007 nm/°C, which is similar to the value obtained by Rappolt and co-workers[38] in a X-ray diffraction study of H_{II} phase lattice parameters as a function of temperature in excess water. The decrease of repeat spacing may be ascribed either to variations of the water region or to modifications of the acyl chains region. However, the present AFM observations do not allow to discriminate between the two scenarios.

In order to analyze the amount of residual water in the obtained H_{II} structures as a function of the preparation temperature, we investigated the OH stretching region of water for samples prepared directly on the ATR silicon crystal following the same procedure used on mica, assuming that the dehydration scheme is the same in both cases. The results for three temperatures (5, 23, and 38 °C) are shown in Figure 4. All the ATR-FTIR spectra have been obtained using nonpolarized illumination and under the condition of thick sample, assuring that all the IR evanescent wave is inside the sample. A comparison between the spectra obtained at 23 and 38 °C highlights that the sample dehydrated at 38 °C results in a lipid aggregate with a lower amount of residual water, with a correspondingly higher amount of lipids probed by the evanescent wave. The OH stretching region is characterized by the presence of mainly three absorption peaks in the 3000−3800 cm^{-1} spectral range. Two major features are represented by a peak around 3400 cm^{-1} and a peak around 3200 cm^{-1}. A weaker peak is also found at around 3600 cm^{-1}. Even if an unambiguous interpretation of the peaks is difficult, the peak at 3200 cm^{-1} is considered representative of bound water, whereas the peak at 3400 cm^{-1} is considered characteristic of water-like organized molecules. According to this interpretation, the signal at 3200 cm^{-1} is indicative of water molecules which interact with the lipid headgroups. The spectrum obtained for the sample prepared at 38 °C shows a relative increase of the peak from ice-like water due to the fact that the smaller water channels are characterized by a decreased relative amount of free water.

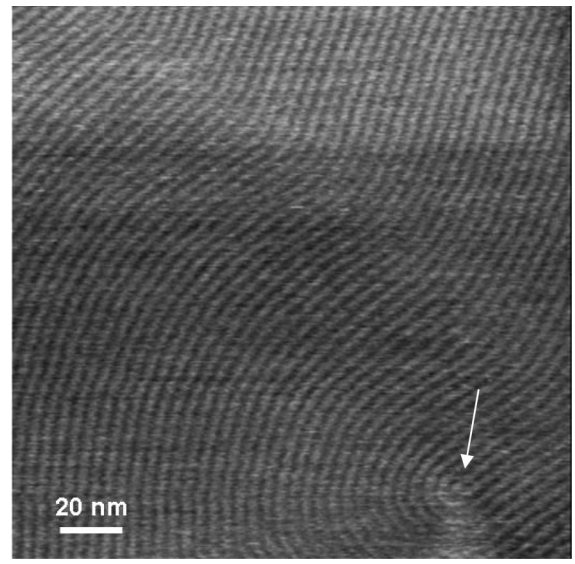

Figure 5. AFM image of a cardiolipin sample dehydrated on a mica surface at 39 °C. Disclination defects are clearly seen (arrow).

According to these results, when a sample is dehydrated at higher temperature a correspondingly higher level of dehydration is obtained by our sample preparation procedure. The observed decrease in the lamellar repeat spacing can so be related to both the decrease of the diameter of the water channel and to the increased disorder of the alkyl chains. However, the signal from the CH_2 stretching vibration of the lipids does not show any significant variation with the sample dehydration temperature, which might suggest that the most important contribution to the variation of the cylinder repeat spacing is due to residual water.

It is noteworthy that the repeat spacing at 5 °C is significantly lower than those observed for temperatures above 25 °C (Table 1), but the amount of the residual water is similar to the 23 °C case. The substantial decrease of repeat spacing may result from the rigid conformation characterizing the acyl chains at low temperatures which might result in an interdigitation process of the chains.

Besides affecting the cylinder repeat spacing, the temperature increase above 25 °C leads to the formation of domains. These can be defined as crystalline regions in which the cylindrical structures are parallel, but their curvature might vary inside the domain. The boundaries of a domain may be defined either as a discontinuity of the cylindrical structures or as a discontinuity of their curvature[39] (tilt boundaries). The progressive increase in temperature leads to a progressive decrease in the average domain area with a parallel increase in their number. The increase in temperature is also associated with a progressive increase in the curvature of cylinder axes that might result in the formation of focal domains[39] or rotational disclination. The phenomenon is shown in Figure 5, where a $+\pi$ disclination in which the director of the cylinders rotate by +180° around one transverse rotation axis of the hexagonal lattice can be seen. This kind of defects has been demonstrated to occur with no additional elastic strain energy in the case of hexagonal phases.[39]

The behavior and organization of defects as a function of temperature, revealed by AFM analysis at nanoscale level, can help to elucidate the mechanism of transition from lamellar to inverted hexagonal phase in view of the results of a molecular dynamics (MD) simulation study of the H_{II} phase formation as a function of temperature and hydration level.[13] According to the results of this study, the transition from the lamellar to the inverted hexagonal phase is characterized by the formation of the so-called "stalks". These are connections between neighboring lamellas which elongate in a cooperative manner thus extending the H_{II} inverted phase. If the stalks are significantly spaced from each other, there is no correlation between them; on the contrary, below a certain distance, the evolution of one stalk correlates with that of the neighboring stalks. The frequency of stalk nucleation increases with temperature and, as a consequence, an increased number of domains and of domain boundaries should also be expected. This conclusion, drawn from MD simulations is experimentally proved by the present observations showing that the average domain area decreases by increasing the temperature with a parallel increase in the number of domain boundaries. The existence of defects characterized by a strong bending of cylinder axes might be the consequence of a collapse of the elastic constant of the cylindrical structures that reduces the energy of formation of these defects. A possible role in the growth of the tubes of the H_{II} phase can be ascribed also to the dehydration pathway. In fact, as dehydration proceeds the number of lipids surrounding a tube should decrease. Due to mass conservation, lipids should be moved along the tube, increasing the tube length. This mechanism could influence the curvature of the resulting tubes. According to this scenario, a higher dehydration level leads to increased cylinder curvature.

The influence of cardiolipin phase behavior on some physical characteristics of the membranes has been considered with attention.[40] It seems therefore of interest to study also the problem from the opposite side, i.e., to explore whether specific chemicals, known to modify the physical properties of natural and artificial membranes,[41,42] might influence the phase behavior of cardiolipin. In this research, the influence of pentachlorophenol (PCP) on the features of the transition from the lamellar to the inverted hexagonal phase of cardiolipin was explored, in view of the effect of this substituted phenol on the electrical conductivity across lipid bilayer membranes.[42]

AFM images of cardiolipin plus PCP samples dehydrated on a mica surface shows that the presence of PCP does not interfere with the formation of the inverted hexagonal phase in cardiolipin−water systems prepared and observed under the conditions used for the controls (Figure 6). As shown in Figure 6, the cylindrical structures lie perfectly parallel to each other with their axes straight over long distance. However, the cylinders are spaced from each other by a value significantly lower than the controls: the repeat spacing is in fact 3.7 nm in the presence of PCP compared to 4.7 nm in the controls. The reduction of the repeat spacing is not associated with other structural defects such as grain boundaries formation or bending of cylinders, a fact that suggests that the frequency of stalk nucleation is not modified by the presence of PCP. Moreover, ATR-FTIR inspection reveals that the water content in the cardiolipin + PCP dehydrated samples is similar to what is obtained for the control samples at the same temperature (data not shown).

The observed reduction of the cylinder repeat spacing may be related to previous findings obtained by Raman spectroscopy showing that PCP causes significant configurational changes of

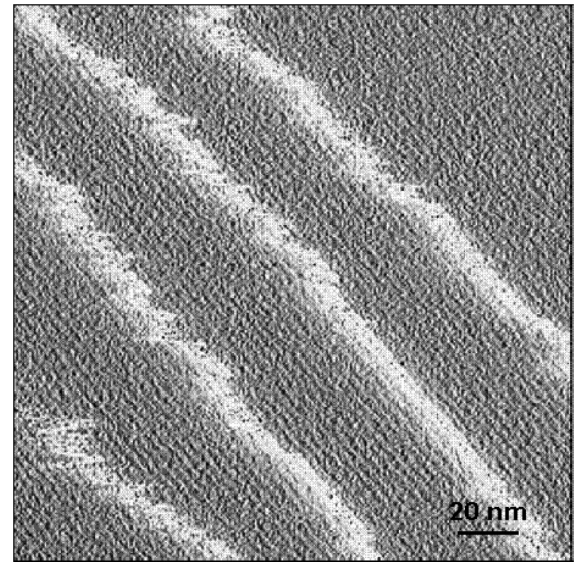

Figure 6. AFM image of a sample of cardiolipin + PCP dehydrated on a mica surface. Crystal planes characterized by the presence of straight cylinders of the H_{II} phase are clearly visible.

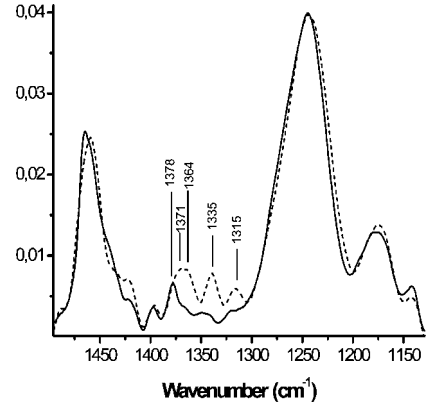

Figure 7. FTIR spectra of a cardiolipin (solid line) and cardiolipin + PCP (dashed line) in the CH_2 wagging modes and wagging progression region.

the acyl chains by increasing the number of gauche rotamers.[43,44] In fact, an increase of acyl chains disorder is associated to a reduction of their length that in turn results in a decrease of the repeat spacing of cylinders observed by AFM. To corroborate this hypothesis, the effect of PCP on cardiolipin molecules was investigated by FTIR analysis. The symmetric CH_2 stretching peak for cardiolipin in the presence of PCP shows an increase in frequency of about 1 cm^{-1} with respect to pure cardiolipin. This type of spectral modification for the CH stretching absorption is generally attributed to an enhanced state of disorder in the acyl chains. However, the correlation between the two phenomena is only qualitative and no direct proportionality between the frequency increase and the number of new gauche rotamers can be established. Figure 7 compares the spectra of cardiolipin in the absence and the presence of PCP in the CH_2 wagging modes and wagging progression region. In samples of cardiolipin added with PCP, localized CH_2 wagging modes are observed in the 1340−1370 cm^{-1} region. A peak at 1378 cm^{-1} corresponding to the methyl umbrella is observed in both spectra, but additional more intense peaks are observed at 1364 and 1335 cm^{-1} in the cardiolipin + PCP spectrum. These localized absorption peaks can be associated to bond conformational states corresponding to kinks and gauche conformers. It is worth noting that the spectrum of PCP itself is characterized

by absorption peaks in the same region. A theoretical and experimental study on PCP by infrared spectroscopy has in fact demonstrated that the most intense absorption peaks of PCP are localized at 1382 and 1302 cm^{-1}.[45] In our study, the peaks at 1315 and 1371 cm^{-1}, which are not found in pure cardiolipin spectra, can be attributed to PCP interacting with cardiolipin. If this conclusion is proved to be true, it can be inferred that PCP molecules partition in the hydrophobic region of the lipid assembly, causing an increase of gauche conformers and, as a consequence, a shortening of the acyl chains. Therefore, the changes in dimension of repeat spacing of cylinders seen by AFM may be explained as a consequence of changes in the structural order of hydrocarbon chains.

An additional important consequence of transition of a CH_2 group from a trans to a gauche conformation is the bending of CH_2 chain with the formation of unoccupied interchain space. This "free volume" is essential for determining important physical parameters including diffusion properties and electrical conductivity.

Conclusions

The aim of the present AFM study was to quantitatively characterize the topographic features of the inverted hexagonal phase of cardiolipin caused by dehydration at different temperatures or by the presence of chemicals. The spatial resolution attained allowed quantitative measurements of packing parameters and provided direct experimental evidence of nanoscale defect formation in the ordered aggregates studied.

The AFM observations confirm that cardiolipin upon dehydration from a lipid water solution adopts the inverted hexagonal phase[26] and show that the geometrical parameters of the H_{II} phase depend on the temperature at which the dispersions are prepared and dehydrated. The results of the analysis of the same samples by FT-IR techniques corroborate the interpretation derived from the AFM images as to the packing geometry of cardiolipin assemblies.

The variation of temperature from 25 to 39 °C is associated to a decrease of cylinder repeat spacing. This phenomenon might be related to both an increase in number of gauche conformers in cardiolipin acyl chains caused by temperature and to the variation of residual water in the H_{II} tubes. Moreover, the increase of temperature above 25 °C causes the formation of nanoscale defects. The analysis of how defects are formed and evolve provides experimental support to the conclusions drawn from a molecular dynamics study on the mechanisms of H_{II} phase formation upon dehydration of a phospholipid water dispersion.[13] In fact, it has been observed that the formation of the H_{II} phase starts with the establishment of stalk connections which elongate cooperatively in a linear manner. The frequency of stalk formation increases with temperature resulting in an increasing number of domains separated by grain boundaries.

As revealed by the observations by both AFM and FT-IR techniques, the presence of pentachlorophenol during sample preparation and dehydration does not inhibit the formation of the H_{II} phase, but causes a substantial reduction of the cylinder repeat spacing as compared to the controls at the same temperature. This may indicate that the PCP molecules interacting with the hydrophobic region of cardiolipin alter the structural order of hydrocarbon chains.

The visualization of molecular scale defects in the lyotropic induced phase transition of cardiolipin from the lamellar phase to the inverted hexagonal phase can be of interest also in the elucidation of the transition mechanism and intermediates, also in light of the fact that cardiolipin might be involved in intermembrane contacts between the inner and outer mitochondrial membranes. Moreover, the possibility of assembling stable multibilayers on a solid support in excess water and the implementation of temperature controlled AFM could open the perspective to the dynamic study in real space of thermotropic phase transitions to the inverted hexagonal phase.[46]

References and Notes

(1) Seddon, J. M.; Templer, R. H. Polymorphism of Lipid-Water systems. In *Handbook of Biological Physics*; Lipowsky, R., Sackmann, E., Eds.; Elsevier Science BV: Amsterdam, 1995.

(2) Luzzati, V. *Biological membranes*; Chapman, D., Ed.; Academic Press: London, 1968; pp 71−123.

(3) Seddon, J. M. *Biochim. Biophys. Acta* **1990**, *1031*, 1–69.

(4) Van den Brink-van der Laan, E.; Killian, J. A.; de Kruijff, B. *Biochim. Biophys. Acta* **2004**, *1666*, 275–288.

(5) Israelachvili, J. N. *Intermolecular and Surfaces Forces*, 2nd ed.; Academic Press: New York, 1991.

(6) Gruner, S. M. *Proc. Natl. Acad. Sci. U.S.A.* **1985**, *82*, 3665–3669.

(7) Kirk, G. L.; Gruner, S. M.; Stein, D. L. *Biochemistry* **1984**, *23*, 1093–1102.

(8) Boggs, J. M. *Biochim. Biophys. Acta* **1987**, *906*, 353–404.

(9) Turner, D. C.; Gruner, S. M. *Biochemistry* **1992**, *31*, 1341–1355.

(10) Epand, R. M. *Chem. Phys. Lipids* **1996**, *81*, 101–104.

(11) Siegel, D. P.; Epand, R. M. *Biophys. J.* **1997**, *73*, 3089–3111.

(12) Ortiz, A.; Killian, J. A.; Verkleij, A. J.; Wilscht, J. *Biophys. J.* **1999**, *77*, 2003–2014.

(13) Marrink, S. J.; Mark, A. E. *Biophys. J.* **2004**, *87*, 3894–3900.

(14) Vögler, O.; Casas, J.; Capò, D.; Nagy, T.; Borchert, G.; Martorell, G.; Escribà, P. V. *J. Biol. Chem.* **2004**, *279*, 36540–36545.

(15) Yang, Q.; Alemany, R.; Casas, J.; Kitajka, K.; Lanier, S. M.; Escribà, P. V. *Mol. Pharmacol.* **2005**, *68*, 210–217.

(16) Rauch, J.; Caffrey, M. *Proc. Natl. Acad. Sci. U.S.A.* **1990**, *87*, 4112–4114.

(17) Liang, H.; Harries, D.; Wong, G. C. L. *Proc. Natl. Acad. Sci. U.S.A.* **2005**, *102*, 11173–11178.

(18) Koynova, R.; Wang, L.; MacDonald, R. C. *Proc. Natl. Acad. Sci. U.S.A.* **2006**, *103*, 14373–14378.

(19) Siegel, D. P.; Epand, R. M. *Biophys. J.* **1997**, *73*, 3089–3111.

(20) Mabrey, S.; Sturtevant, J. M. *Proc. Natl. Acad. Sci. U.S.A.* **1979**, *73*, 3862–3866.

(21) de Kruijff, B.; Rietveld, A.; van Echteld, C. J. *Biochim. Biophys. Acta* **1980**, *600*, 597–606.

(22) Mantsch, H. H.; McElhaney, R. N. *Chem. Phys. Lipids* **1991**, *57*, 213–226.

(23) Dufrêne, Y. F.; Lee, G. U. *Biochim. Biophys. Acta* **2000**, *1509*, 14–41.

(24) Tokumasu, F.; Jin, A. J.; Dvorak, J. A. *J. Electron Microsc.* **2002**, *51*, 1–9.

(25) Kaasgaard, T.; Leidy, C.; Crowe, J. H.; Mouritsen, O. G.; Jorgensen, K. *Biophys. J.* **2003**, *85*, 350–60.

(26) Alessandrini, A.; Valdrè, G.; Valdrè, U.; Muscatello, U. *Chem. Phys. Lipids* **2007**, *146*, 111–124.

(27) Rand, R. P.; Sengupta, S. *Biochim. Biophys. Acta* **1972**, *255*, 484–492.

(28) McAuley, K.; Fyfe, P. K.; Ridge, J. P.; Isaacs, N. W.; Cogdell, R. J.; Jones, M. R. *Proc. Natl. Acad. Sci. U.S.A.* **1999**, *96*, 14706–14711.

(29) Choi, S.; Swanson, J. M. *Biophys. Chem.* **1995**, *54*, 271–278.

(30) Smejtek, P.; Hsu, K.; Perman, W. H. *Biophys. J.* **1976**, *16*, 319–336.

(31) Haines, T. H.; Dencher, N. A. *FEBS Lett.* **2002**, *528*, 35–39.

(32) Koshkin, V.; Greenberg, M. L. *Biochem. J.* **2000**, *347*, 687–691.

(33) Putman, C. A.; van der Werf, K. O.; de Grooth, B. G.; van Hulst, N. F.; Greve, J.; Hansma, P. K. *SPIE Scanning Probe Microsc.* **1992**, *1693*, 198–204.

(34) Goormaghtigh, E.; Raussens, V.; Ruysschaert, J.-M. *Biochim. Biophys. Acta* **1999**, *1422*, 105–185.

(35) Dave, N.; Lorenz-Fonfria, V. A.; Leblanc, G.; Padros, E. *Biophys. J.* **2008**, *94*, 3659–3670.

(36) Binder, H.; Anikin, A.; Lantzsch, G.; Klose, G. *J. Phys. Chem. B* **1999**, *103*, 461–471.

(37) Casal, H. L.; Mantsch, H. H. *Biochim. Biophys. Acta* **1984**, *779*, 381–401.

(38) Rappolt, M.; Hickel, A.; Bringezu, F.; Lohner, K. *Biophys. J.* **2003**, *84*, 3111–3122.

(39) Kleman, M. *J. Phys. (Paris)* **1980**, *41*, 737–745.

(40) Ortiz, A.; Killian, J. A.; Verkleij, A. J.; Wilschut, J. *Biophys. J.* **1999**, *77*, 2003–2014.

(41) Mitchell, P.; Moyle, J. In *Biochemistry of Mitochondria*; Slater, E. C., Kaninga, Z., Wojtczak, L., Eds.; Academic Press: London, 1967.

(42) Smejtek, P.; Hsu, K.; Perman, W. H. *Biophys. J.* **1976**, *16*, 319–336.

(43) Fini, G.; Pasquali-Ronchetti, I. *Membr. Biochem.* **1981**, *4*, 119–128.

(44) Pasquali-Ronchetti, I.; De Aloysio, G.; Ghisellini, M.; Fini, G. *J. Submicrosc. Cyt.* **1980**, *12*, 43–59.

(45) Czarnik-Matusewicz, B.; Chandra, A. K.; Tho, N. M.; Zeegers-Huyskens, T. *J. Mol. Spectrosc.* **1999**, *195*, 308–316.

(46) Picas, L.; Montero, M. T.; Morros, A.; Oncins, G.; Hernández-Borrell, J. *J. Phys. Chem. B* **2008**, *112*, 10181–10187.

JP809705D